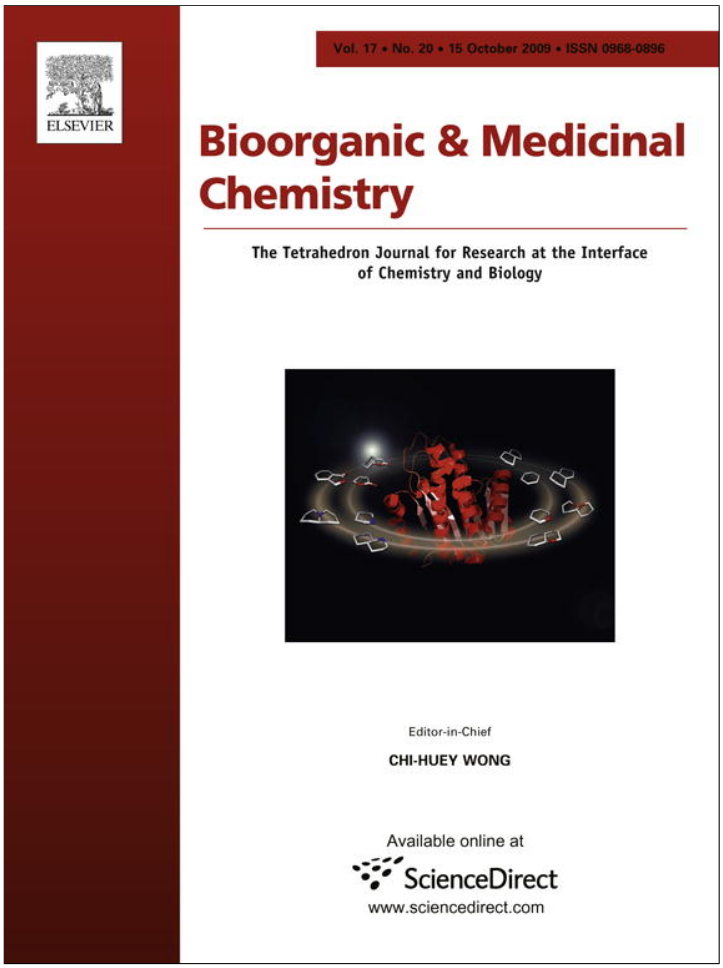

Bioorganic & Medicinal Chemistry 17 (2009) 7145–7155

Contents lists available at ScienceDirect

Bioorganic & Medicinal Chemistry

journal homepage: www.elsevier.com/locate/bmc

Synthesis and biological evaluation of 14-(aminoalkyl-aminomethyl)-aromathecins as topoisomerase I inhibitors: Investigating the hypothesis of shared structure–activity relationships

Maris A. Cinelli [a], Brenda Cordero [a], Thomas S. Dexheimer [b], Yves Pommier [b], Mark Cushman [a,*]

[a] Department of Medicinal Chemistry and Molecular Pharmacology, School of Pharmacy and Pharmaceutical Sciences, and the Purdue Cancer Center, Purdue University, West Lafayette, IN 47907, USA
[b] Laboratory of Molecular Pharmacology, Center for Cancer Research, National Cancer Institute, Bethesda, MD 20892-4255, USA

ARTICLE INFO

Article history:
Received 9 July 2009
Revised 22 August 2009
Accepted 29 August 2009
Available online 6 September 2009

Keywords:
Topoisomerase I
Aromathecins
Anticancer
Polyamine

ABSTRACT

The aromathecin topoisomerase I (top1) inhibitors offer promising scaffolds for the development of novel cancer chemotherapeutics. They are 'composites' of the camptothecin and indenoisoquinoline top1 inhibitors. Interestingly, some structure–activity relationship (SAR) overlap between the aromathecins and the indenoisoquinolines has been observed. For both classes, placement of certain polar groups in similar regions of the heteroaromatic system improves top1 inhibitory and antiproliferative activities. A series of water-soluble aromathecins substituted at position 14 with diaminoalkanes of various lengths has been prepared. These compounds all possess similar antiproliferative potency, but a general trend is observed: aromathecins with longer diaminoalkane substituents (>6 carbons) possess lower anti-top1 activity than their smaller counterparts (2–4 carbons), presumably as a result of unfavorable hydrophobic interactions. This trend is also noted with the indenoisoquinolines, revealing additional SAR overlap that supports the hypothesis that there is a 'universal' top1 inhibitor SAR.

1. Introduction

Topoisomerase I (top1) breaks one strand of double-stranded DNA. The cleaved strand then rotates around the uncleaved strand, resulting in relaxation of DNA supercoils necessary for replication and transcription. The broken DNA strand then re-ligates and relaxed DNA is released.[1,2] Top1 is overexpressed in human cancers,[3,4] and interest in top1 as a therapeutic target was stimulated by the isolation of camptothecin (**1**) and the later development of topotecan (**2**) and irinotecan (**3**),[5] which inhibit the DNA religation reaction by intercalating at the cleavage site, eventually leading to apoptosis (Fig. 1).[2,6–9]

Topotecan and irinotecan are potent anticancer drugs, but are limited by reversibility of their ternary drug–DNA–enzyme complexes, which necessitates long infusion times for maximum therapeutic benefit. Drug efflux pumps[10] and resistance mutations[11,12] also limit their efficacy. Side effects include diarrhea, immune suppression, and hemorrhagic cystitis.[1,13,14] The E-ring hydroxylactone exists in equilibrium with an open hydroxyacid form that binds to human serum albumin, thus compromising bioavailability.[1,15–18]

Alternative top1 inhibitors have been based on natural products such as luotonin A (**4**)[19] and the indolocarbazoles.[20] Optimization of the latter class has provided edotecarin (**5**).[13,21] The indenoisoquinolines, such as **6**, are synthetic compounds based on the lead NSC 314622 (**7**).[22–25] Two indenoisoquinolines are slated to begin clinical trials at the NIH.[26]

The 12*H*-5,11a-diazadibenzo[*b,h*]fluoren-11-one system, called 'rosettacin' (**8**)[27] when unsubstituted and 'aromathecin' when substituted, was first discovered in the natural product 22-hydroxyacuminatine (**9**).[28] This system is an analogue of camptothecin, with the E-ring lactone replaced by a benzene ring. As such, the system is a 'hybrid' of the camptothecin and indenoisoquinoline systems. Although initial attempts to develop aromathecins were less than fruitful,[29] subsequent efforts led to the synthesis of the more promising 14-substituted aromathecins.[30] These compounds, substituted with amino alcohols and nitrogen heterocycles, possess both greater anti-top1 and antiproliferative activity than rosettacin and a greater ability to inhibit top1 than 22-hydroxyacuminatine.

Interestingly, indenoisoquinoline top1 inhibitory activities are increased by the same substituents (ethanolamine, morpholine, imidazole, etc.)[23,24] that increase the activity of the aromathecins.[23,24] Molecular modeling and crystallography[8] indicate that the lactam region of the indenoisoquinoline system (where these substituents are located) overlaps spatially with both the 7-position of

* Corresponding author. Tel.: +1 765 494 1465; fax: +1 765 494 6790.
E-mail address: cushman@pharmacy.purdue.edu (M. Cushman).

0968-0896/$ - see front matter © 2009 Elsevier Ltd. All rights reserved.
doi:10.1016/j.bmc.2009.08.066

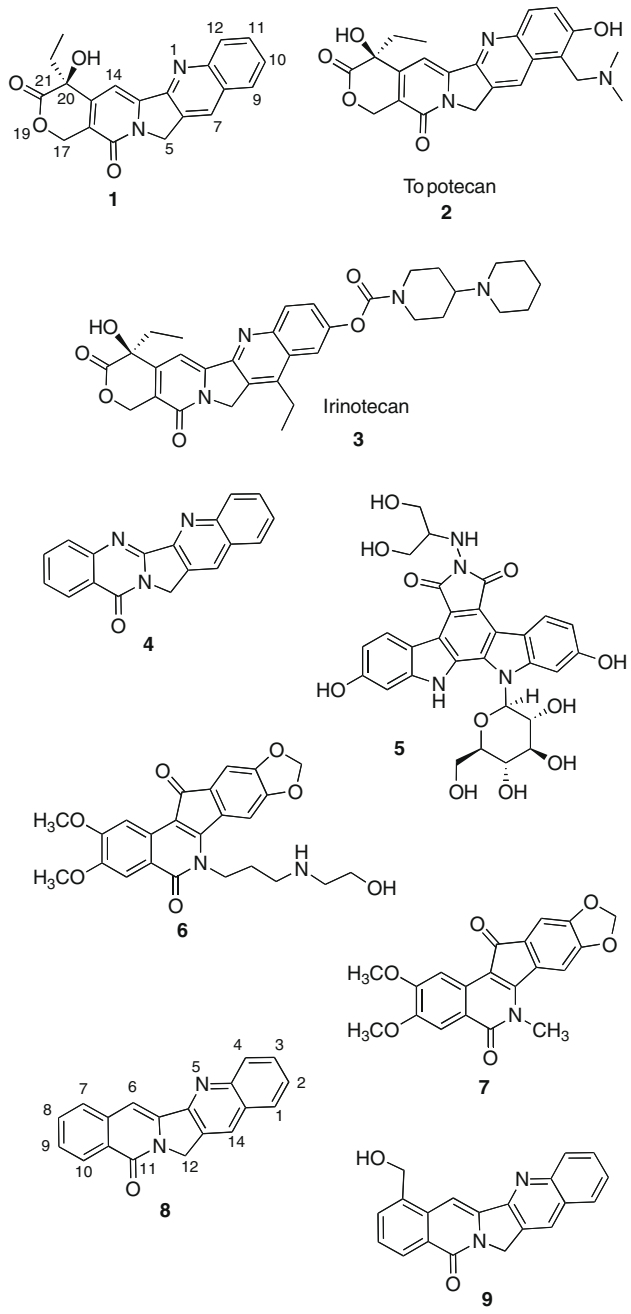

Figure 1. Representative top1 inhibitors.

camptothecin and the 14-position of the aromathecin system in their respective ternary cleavage complexes. These substituents likely project into the DNA major groove in the cleavage complex.[30] This spatial overlap suggests a significant degree of *structure–activity relationship overlap* between these two systems.[8] The similar substituent effects suggest that other aspects of the indenoisoquinoline SAR might be 'translated' to the aromathecin system.

Indenoisoquinolines substituted with di- and polyamines are potent top1 inhibitors.[31,32] It is known in general that di- and polyamine conjugates are effective 'DNA-targeting' moieties for many classes of intercalating and anti-top1 compounds.[31–35] In 2007, Morrell et al. determined that diamines with two- to four-carbon spacers were optimal substituents for bioactivity when placed on indenoisoquinolines.[31] The question as to whether this SAR trend could also be applied to aromathecins served as a rationale for the synthesis of 14-[(aminoalkyl)-aminomethyl)aromathecins **53–63**.

2. Chemistry

There are several routes known to the aromathecin system, including the condensation of pyrroloquinoline with phthalides,[28,29] pyridone benzannulation and Heck coupling,[36] and variants of the Friedlander condensation.[30,37] Our synthesis of 14-substituted aromathecins proceeds through pyrroloquinolinedione **16** (Scheme 1), first prepared by Shamma and Novak in 1968.[38] Intermediate **11** was prepared by the facile decarboxylation of commercially available *trans*-4-hydroxy-L-proline (**10**).[39] Condensation of **11** with 3-chlorophthalide **13** (easily prepared from 2-carboxybenzaldehyde **12**)[40] yielded the hydroxyamide **14**. Previously, this compound was oxidized and cyclized to **16** via oxidation with pyridinium dichromate and subsequent treatment with polyphosphoric acid.[30] An improved variant of this oxidation–cyclization has been discovered. Subjecting **14** to Swern conditions and a brief reflux period affords **16** rapidly (via intermediate **15**). These new conditions furnish the key intermediate in improved yield (50–60%) without recourse to heavy metal oxidants and extensive purification. 14-Chloromethylaromathecin (**19**)[30] was prepared by Friedlander condensation of ketone **16** with aminoacetophenone **18** (Scheme 2). Compound **18** was in turn prepared from aniline (**17**) and chloroacetonitrile using the Sugasawa modification of the Friedel–Crafts acylation.[41,42]

Compound **19** undergoes S_N2 displacement easily at its benzylic chloride (Scheme 3). The diamine moieties were installed as their mono-Boc-protected carbamates to prevent polymerization under the displacement conditions and to aid in purification. Following Morrell et al.'s procedure, diamines **20–30** were readily protected using Boc_2O to afford the carbamates **31–41**.[31] Treatment of **19** with excess protected diamine in DMSO at room temperature afforded the aromathecin carbamates **42–52**. Compounds **42–52** were readily deprotected using methanolic HCl either in chloroform, or in the case of diaminoheptane analogue **47**, refluxing benzene, to yield the water-soluble aromathecin salts **53–63**. Elemental analysis proved these analogues were trihydrochloride salts, protonated on both amines and the quinoline nitrogen.

3. Results and discussion

Aromathecin analogues were assayed for cytotoxic activity in the National Cancer Institute's Developmental Therapeutics

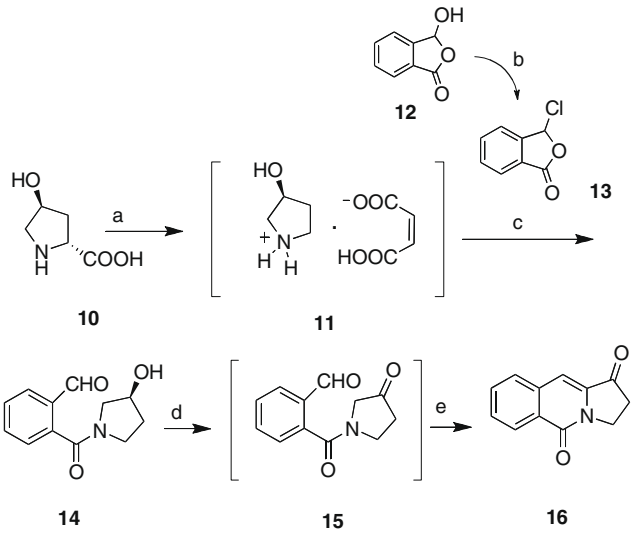

Scheme 1. Reagents and conditions: (a) (i) cat. 2-cyclohexen-1-one, cyclohexanol, reflux; (ii) maleic acid, EtOAc, rt; (b) $FeCl_3$, $SOCl_2$, reflux; (c) MeOH, Et_3N, rt; (d) (i) DMSO, $(COCl)_2$, CH_2Cl_2, −78 °C; (ii) Et_3N, −78 °C–rt; (e) reflux.

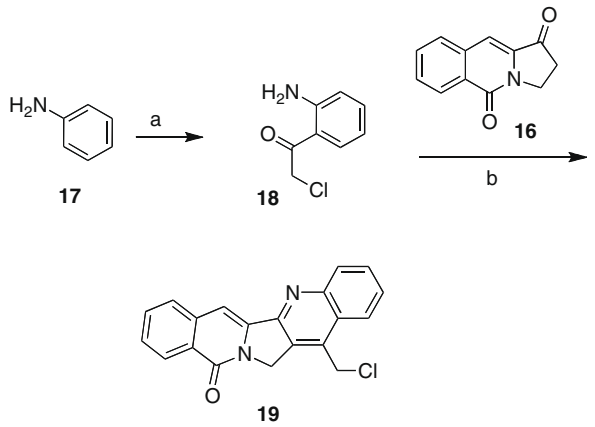

Scheme 2. Reagents and conditions: (a) (i) $BCl_3{\cdot}Me_2S$, 1,2,-dichloroethane, 0 °C; (ii) chloroacetonitrile, $AlCl_3$, reflux; (iii) 2 M HCl, reflux; (b) *p*-TsOH, toluene, reflux.

screen.[43,44] Although some highly potent Boc-polyaminocamptothecins have been reported,[33] indenoisoquinoline carbamates are largely inactive.[31,45] Therefore, the intermediate carbamates **42–52** were not tested.

Compounds accepted for testing were assayed against approximately 60 cell lines originating from various human tumors.[43,44] Following an initial one-dose assay (at 10^{-5} M), selected compounds were tested at five concentrations ranging from 10^{-8} to 10^{-4} M. Cytotoxicity results are reported as GI_{50} values for selected cell lines from each subpanel, and overall antiproliferative potency is quantified as a mean-graph midpoint (MGM) in Table 1. The MGM is a measure of the average GI_{50} against all cell lines tested, where compounds whose GI_{50} values fall outside the concentration range tested (10^{-8}–10^{-4} M) are assigned GI_{50} values of either 10^{-8} M or 10^{-4} M. For comparative purposes, the activities of camptothecin (**1**), the indenoisoquinolines **6** (MJ-III-65),[1,23,25] and NSC314622 (**7**),[22] and rosettacin (**8**) are reported.

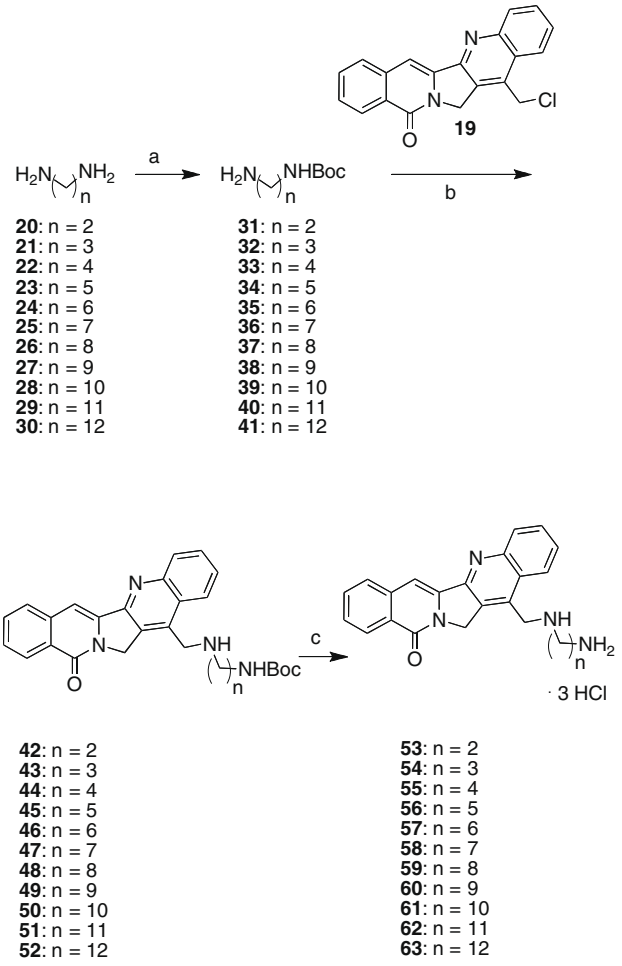

Scheme 3. Reagents and conditions: (a) Boc_2O, $CHCl_3$, rt; (b) DMSO, rt; (c) 3 M HCl, MeOH, $CHCl_3$, rt or 3 M HCl, MeOH, benzene, reflux (47).

Top1 inhibition was evaluated by measurement of top1-dependent DNA cleavage at four concentrations, and inhibition data are expressed semiquantitatively using the following rubric: 0, no inhibitory activity; +, between 20% and 50% the activity of 1 μM camptothecin (**1**); ++, between 50% and 75% the activity of 1 μM camptothecin; +++, between 75% and 100% the activity of 1 μM camptothecin; and ++++, equipotent to or more potent than 1 μM camptothecin. Top1 inhibitory data for **1** and **6–8** are also included in Table 1.

Compounds **53–54**, **56–57**, **59**, **61**, and **63** were assayed for antiproliferative activity. These aromathecins, on average, display higher antiproliferative potency than many of the 14-substituted aromathecins previously investigated.[30] These water-soluble salts are more easily formulated than many of the free bases previously tested. In addition, it is well known that positively charged substituents improve DNA targeting, binding, and intercalative potential through simple electrostatic complementarity to negatively charged DNA. This effect has been observed for camptothecins, indenoisoquinolines, acridines, and other polyaromatic hydrocarbon-based systems when substituted with di- and polyamines, amidines, and guanidines.[31–35,45–47]

Interestingly, with the exception of compound **61**, little variance in antiproliferative activity is observed in the compounds tested, regardless of side chain length. Anomalously, compound **61** actually *induced* cell growth by approximately 30% at a concentration of 10 μM in the initial one-concentration assay, although both the large observed variance between individual cell lines and the general trend among the rest of this series indicate that this result may be an artifact of testing. For indenoisoquinolines and other compounds, it was observed that an increasing C log *P* correlated well with decreasing cytotoxicity, possibly as a result of poor solubility, inefficient DNA-targeting, or other hydrophobic effects.[31] There is no correlation for aromathecins, however; compounds **53** and **63** are equipotent, and compound **57**, more hydrophobic than **53**, is more active.

For top1 inhibition, the shorter diaminoalkanes confer good anti-top1 activity upon the aromathecin core, inducing top1-mediated DNA breakage as shown in Figure 2. These compounds induce DNA cleavage patterns resembling those caused by both camptothecins and indenoisoquinolines. Activity generally decreases with increasing side-chain length, however. With the exception of **56**, up to six atoms between proximal and distal amines are tolerated readily for aromathecins. Activity decreases beyond this length, and compounds with ten or more carbons are completely inactive. An *identical* trend is noted for indenoisoquinolines, complete with compounds derived from 1,5-pentanediamine possessing significantly less anti-top1 activity than those derived from 1,6-hexanediamine.[31] It is unknown why the pentanediamino compounds possess such low anti-top1 activity.

It has been confirmed by X-ray crystallography that the lactam substituents of indenoisoquinolines project into the major groove of the ternary complex.[8] Hypothetical models predict that the 14-position substituents of aromathecins project into the same region, where they likely interact favorably with water and amino acids such as Asn352.[48,49] Figure 3 shows a hypothetical model of compound **53**, the most potent top1 inhibitor from this series,

Table 1
Cytotoxicities and topoisomerase I inhibitory activity of 14-diamine-substituted aromathecin analogues

Compd	Cytotoxicity (GI_{50} in μM)[a]								MGM[b]	Top 1 cleavage[c]
	Lung HOP-62	Colon HCT-116	CNS SF-539	Melanoma UACC-62	Ovarian OVCAR-3	Renal SN12C	Prostate DU-145	Breast MDA-MB-435		
1	0.01	0.03	0.01	0.01	0.22	0.02	0.01	0.04	0.040 ± 0.019	++++
6	0.02	0.10	0.04	0.03	0.5	<0.01	<0.01	0.79	0.11	++++
7	1.3	35	41	4.2	73	68	37	96	20.0	++
8	68.2	32.7	66.7	97.2	39.8	>100	>100	41.8	58.9	++
53	1.4	1.5	8.3	12.6	1.7	1.5	1.4	11.0	2.8 ± 0.11	+++
54	9.8	1.5	4.9	4.8	1.4	2.1	1.1	6.8	2.1 ± 0.38	++(+)
55[e]	—	—	—	—	—	—	—	—	—	+++
56	2.6	3.2	7.2	1.9	8.1	3.2	1.1	12.6	2.6 ± 1.65	+
57	1.2	0.63	0.74	2.0	1.4	0.51	0.33	1.5	1.0	++(+)
58[e]	—	—	—	—	—	—	—	—	—	++
59	2.8	1.8	1.9	1.8	2.5	1.8	1.1	3.1	1.9	+
60[e]	—	—	—	—	—	—	—	—	—	+
61[d]	—	—	—	—	—	—	—	—	—	0
62[e]	—	—	—	—	—	—	—	—	—	0
63	6.5	2.0	1.8	1.9	1.9	2.5	2.0	1.7	2.6	0

[a] The cytotoxicity GI_{50} values are the concentrations corresponding to 50% growth inhibition.
[b] Mean graph midpoint for growth inhibition of all human cancer cell lines successfully tested, ranging from 10^{-8} to 10^{-4} M.
[c] Compound-induced DNA cleavage due to top1 inhibition is graded by the following rubric relative to 1 μM camptothecin: 0, no inhibitory activity; +, between 20% and 50% activity; ++, between 50% and 75% activity; +++, between 75% and 100% of activity; ++++, equipotent.
[d] Not selected for further testing; refer to text for details.
[e] Declined for one-dose cytotoxicity testing by the NCI.

in ternary complex with top1 and DNA. The aromathecin core is proposed to intercalate between the base pairs flanking the top1-induced cleavage site, where the quinoline nitrogen faces toward the minor groove and may interact with Arg364. Although it is out of hydrogen-bonding distance (4.47 Å) in this model, this contact is closer in other aromathecin models,[30] as well as in camptothecin and topotecan crystal structures,[7,8] and hydrogen bonding might still be possible in the present case with induced fit. The diamine side chain projects into the major groove, where it is proposed to hydrogen bond with a flanking nucleobase. Water molecules likely participate in these interactions, and this hypothetical network of water-mediated H-bonds and polar contacts with the positively charged amines is shown in Figure 4. In this well-solvated environment, it can be seen how increasingly hydrophobic side-chains (such as those over eight carbons as in **60**–**63**) would yield unfavorable interactions by possibly disturbing this intricate network of water molecules. Larger side chains may also be hindered by steric or entropic factors.

The fact that aromathecin diamines behave in a manner that is identical to analogous indenoisoquinolines with regard to top1 inhibition lends additional support to the proposed binding mode (where the 14-position faces the major groove). This behavior can be rationalized through molecular modeling. Figure 5 depicts the ligands **53** and **64** (Fig. 6) in an overlay of the hypothetical

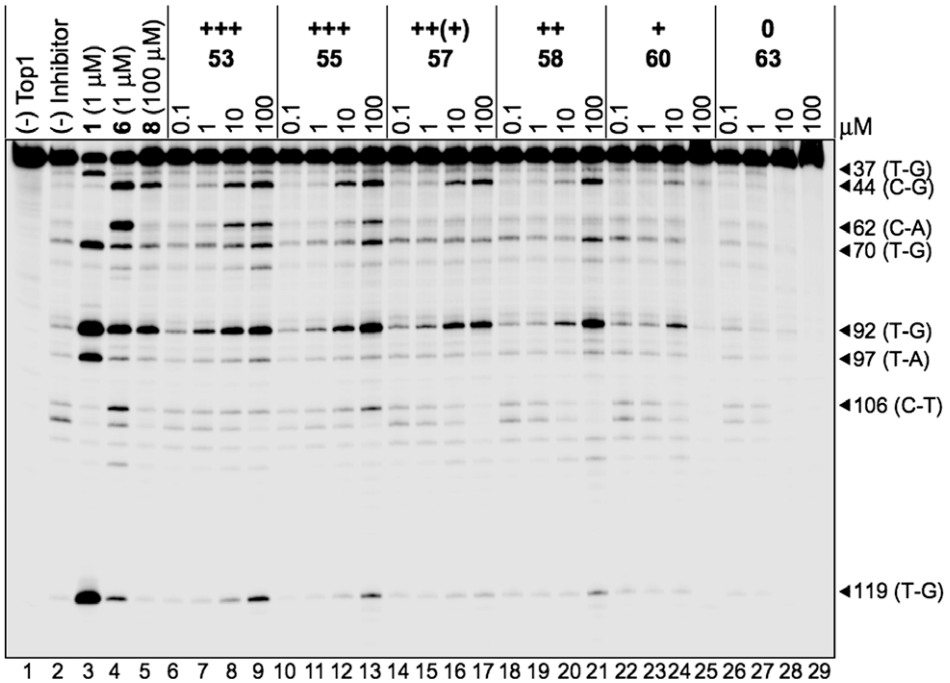

Figure 2. Top1-mediated DNA cleavage induced by aromathecins **53**, **55**, **57**, **58**, **60**, and **63**. Lane 1: DNA alone; lane 2: Top1 alone; lane 3: **1**, 1 μM; lane 4: **6**, 1 μM; lane 5: **8**, 100 μM; lanes 6–29: **53**, **55**, **57**, **58**, **60**, and **63** at 0.1, 1, 10, and 100 μM, respectively, from left to right. Numbers and arrows on right indicate arbitrary cleavage site positions.

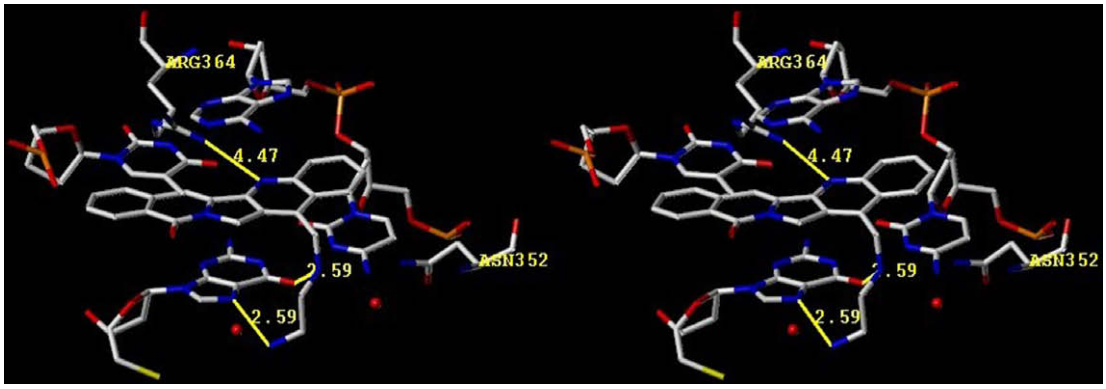

Figure 3. Hypothetical model of aromathecin **53** in ternary complex with top1 and DNA showing proposed hydrogen bonds. Water molecules are red spheres; distances are between heavy atoms. The stereoview is programmed for wall-eyed viewing.

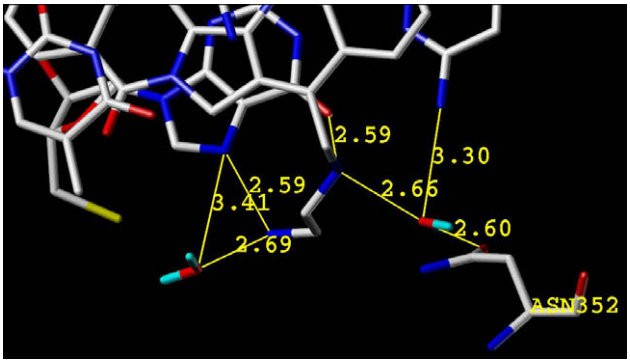

Figure 4. Hypothetical model of water-mediated hydrogen bonds and polar contacts between diaminoethyl side chain of aromathecin **53**, Asn352, and DNA base pairs. Water molecules are indicated in red, other structures are colored by atom type. Distances are between heavy atoms.

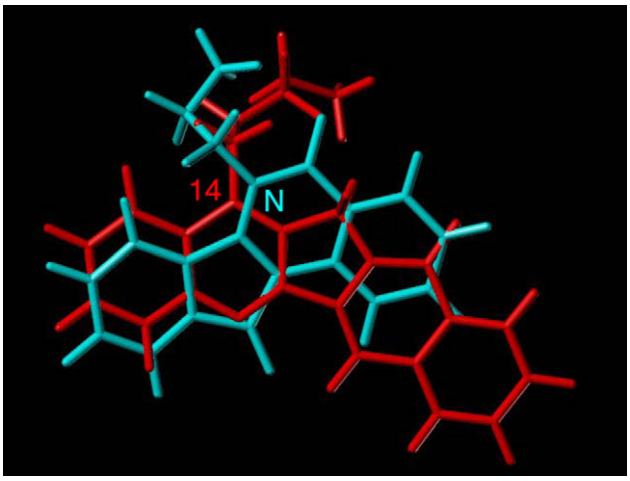

Figure 5. Ligand overlay of hypothetical ternary complex models of aromathecin **53** (green) and indenoisoquinoline **64** (cyan). The positions of the lactam nitrogen and 14-position are also shown in their respective colors.

models of their ternary complexes.[8,31] The aromatic regions sit approximately in the same position, the side chains occupy identical regions spatially, and both interact with Asn352 and water molecules (not shown).

It is worth noting the disparities between cytotoxicity and top1 inhibition across this analogue series. Such a disparity is not unprecedented and has been previously observed in indenoisoquinolines,[23,31] anthracenes,[46] camptothecins,[33] and aromathecins[30] alike. Dallavalle et al. propose that beyond Coulombic attraction of the drugs to DNA, the cellular pharmacology of positively-charged 'polyamine' conjugates is an exceedingly complex interplay of intrinsic molecular structure, hydrophobicity, and subcellular localization.[33] This is consistent with Morrell et al.'s hypotheses that differential ADME properties are responsible for these discrepancies.[31]

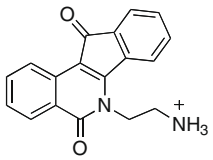

64

Figure 6. Structure of Indenoisoquinoline **64**.

If such a disparity exists between cytotoxicity and top1 inhibition, then what is the macromolecular target of compounds such as **56** and **63** that possess little anti-top1 activity? A COMPARE analysis was performed on data from compound **56**, which, with its low anti-top1 activity, is effectively a 'targetless' aromathecin. The NCI's COMPARE algorithm attempts to correlate the antiproliferative potency of a compound with a possible target or mechanism of action.[44,50,51] When the data for **56** were used to seed a COMPARE search, the program returned compounds such as amsacrine[47] and teniposide with a moderately high (>0.75) correlation. These compounds act predominantly through inhibition of topoisomerase II (top2). When compounds **56**, **57**, **59**, and **63** were assayed for the ability to induce top2-mediated DNA cleavage, however, little inhibitory activity was found. It is also worth noting that at high concentrations, longer diamines like **60** and **63** suppress the formation of top1-DNA cleavage complexes (as shown in Fig. 3),[31] although the shorter diamines do not. This could indicate that the antiproliferative activity of compounds such as **63** may involve topoisomerase binding or non-specific DNA intercalation. Also, the role of cellular polyamine transporters in the pharmacokinetics of these molecules cannot be discounted.[52]

The high degree of overlap in the SAR at the indenoisoquinoline lactam nitrogen and the aromathecin 14-position, down to specific substituents, is significant, and supports the hypothesis that there is a 'common' or 'universal' structure–activity relationship among different classes of top1 inhibitors. Different substituents have been 'translated' effectively between camptothecins and indenoisoquinolines in optimization of the latter class' indenone ring.[53] This SAR overlap is also seen between camptothecins and

aromathecins in translation of active substituents from the former's 7-position (such as the *N*-methylpiperazine of lurtotecan and camptothecin analogues)[1,17] to the 14-position of aromathecins.[30] There is also overlap between the SARs of indenoisoquinolines, isoquinocinnolinones, and dibenzonaphthyridones in the usage of common lactam and ring substituents.[54,55] Indeed, Staker et al. have described certain structural features common to all effective top1 inhibitors, including major groove substituents, a planar ring that faces the nonscissile strand, and a hydrogen-bond acceptor facing the minor groove.[8] These new results could thus support the translation of other substituents to the aromathecin class to produce novel potent top1 inhibitors.

4. Conclusions

In conclusion, a new series of water-soluble 14-substituted aromathecins bearing diaminoalkanes of various lengths has been synthesized by a facile route beginning with commercially available starting materials. An improved preparation of the key intermediate in aromathecin synthesis is also reported. The analogues were assayed against top1 and various human cancer cell lines. This series contains the most cytotoxic aromathecins synthesized thus far, their improved antiproliferative potency likely due to increased solubility and multiple DNA-targeting positive charges. In general, top1 inhibition decreases with increasing side chain length, likely reflecting the effect of unfavorable hydrophobic clashes in the charged and well-solvated major groove of the ternary complex. Hypothetical models seem to support this assumption, as well as the hypothesis that hydrogen bonding may play a significant role in ternary complex stabilization. No correlation is observed between cytotoxicity and top1 inhibition, however, indicating top1 is not the sole determinant of antiproliferative potency. Interestingly, the top1 inhibition trend is identical to that observed for indenoisoquinolines. In addition to supporting our proposed binding mode, these data indicate additional SAR overlap with this related class of top1 inhibitors, and possibly lend support to the hypothesis that there may be features common to all effective top1 poisons.

5. Experimental

5.1. General procedures

Reagents and solvents were purchased from commercial vendors and were used without further purification. Analytical thin-layer chromatography was performed on Baker-flex silica gel IB2-F plastic-backed TLC plates. Preparative thin-layer chromatography was performed on Analtech silica gel G1200 μM glass plates. Compounds were visualized with both short and long-wavelength UV light. Silica gel flash chromatography was performed using 40–63 μm flash silica gel. Melting points were determined in capillary tubes using a Mel-Temp apparatus and are uncorrected. Infrared spectra were obtained as films on salt plates using $CHCl_3$, $CDCl_3$, or $CHCl_3$/MeOH as the solvent unless otherwise specified, using a Perkin–Elmer Spectrum One FT-IR spectrometer. All spectra are baseline-corrected. ^{1}H NMR spectra were obtained at 300 or 500 MHz, using a Bruker ARX300 and Bruker Avance 500 (QNP and TXI 5 mm probe), respectively. Mass spectral analyses were performed at the Purdue University Campus-Wide Mass Spectrometry Center. ESIMS (electrospray ionization mass spectrometry) was performed using a FinniganMAT LCQ Classic mass spectrometer system. Combustion microanalyses were performed at the Purdue University Microanalysis Laboratory using a Perkin–Elmer Series II CHNS/O model 2400 analyzer and all reported values are within 0.4% of calculated values. Precursor compounds **11**,[39] **13**,[49] **14**,[30] and **18**[41,42] were prepared as previously described and as depicted in Schemes 1 and 2.

5.2. Synthesis of precursors

5.2.1. 2,3-Dihydropyrrolo[1,2-*b*]isoquinoline-1,5-dione (16)[38]

Anhydrous CH_2Cl_2 (170 mL) was cooled, under an argon atmosphere, to −78 °C. DMSO (2.96 g, 37.9 mmol) was added, followed, dropwise, by oxalyl chloride (2.40 g, 18.9 mmol). Upon cessation of gas evolution (10 min), compound **14**[30] (3.78 g, 17.2 mmol), as a solution in CH_2Cl_2 (20 mL), was added slowly, and the resultant opaque off-white solution was stirred for 15 min. Triethylamine (8.69 g, 86 mmol) was added, and the mixture became orange. After stirring for 5 min at −78 °C, the mixture was warmed to room temperature (TLC indicated the presence of **15**), and darkened as cyclization began. The mixture was stirred for 30 min and heated at reflux for 2 h. The black solution was cooled and washed with H_2O (2 × 200 mL). The aqueous layer was extracted with $CHCl_3$ (150 mL). The combined organic layers were washed with H_2O (2 × 200 mL), satd NaCl (200 mL), dried over anhydrous sodium sulfate, treated with decolorizing carbon (1.00 g), and filtered. The filtrate was concentrated to yield a pale-orange microcrystalline solid (2.01 g, 59%) after washing with MeOH (40 mL) and ether (20 mL): mp 180–183 °C (lit.[38] mp 191–192 °C). ^{1}H NMR (300 MHz, $CDCl_3$) δ 8.54 (d, J = 8.1 Hz, 1H), 7.80–7.65 (m, 3H), 7.29 (s, 1H), 4.42 (t, J = 7.0 Hz, 2H), 2.99 (t, J = 7.3 Hz, 2H).

5.2.2. 14-Chloromethyl-12*H*-5,11a-diazadibenzo[*b*,*h*]fluoren-11-one (19)[30]

Compound **16** (0.284 g, 1.43 mmol) and compound **18**[49] (0.291 g, 1.72 mmol) were diluted with toluene (35 mL) and *p*-TsOH (0.272 g, 1.43 mmol) was added. The mixture was heated at reflux (using a Dean–Stark trap to collect azeotroped water) for 17 h. The bright-orange suspension was cooled, concentrated, and diluted with $CHCl_3$ (100 mL). The organic phase was washed with satd $NaHCO_3$ (200 mL) and the aqueous layer was extracted with $CHCl_3$ (100 mL), and the combined organic layers were washed with 5% $NaHCO_3$ and satd NaCl (100 mL each). The solution was dried over anhydrous sodium sulfate and concentrated to yield a yellow amorphous solid (0.425 g, 89%) after washing with MeOH (50 mL): mp 274–280 °C [(dec), lit.[30] mp 270 °C (dec)]. ^{1}H NMR (300 MHz, $CDCl_3$) δ 8.56 (d, J = 8.1 Hz, 1H), 8.27 (d, J = 7.9 Hz, 1H), 8.19 (d, J = 8.2, 1H), 7.84–7.59 (m, 6H), 5.44 (s, 2H), 5.04 (s, 2H).

5.3. General procedure for synthesis of mono-Boc diaminoalkanes 31–41[31]

Boc_2O (0.5 g, 2.29 mmol) was dissolved in $CHCl_3$ (10 mL) and added dropwise to the diamine (11.4 mmol), dissolved in $CHCl_3$ (50 mL). The reaction mixture was allowed to stir overnight at room temperature. The solution was concentrated, adsorbed onto SiO_2, and purified by flash column chromatography (SiO_2), eluting with 10% MeOH–1% Et_3N in $CHCl_3$ to afford the mono-Boc-protected diamines in acceptable purity after drying in vacuo.

5.3.1. Mono-Boc-1,2-diaminoethane (31)

From **20**, the general procedure afforded the desired product as a clear, pale-yellow viscous oil (0.382 g, 100% with minor impurities): ^{1}H NMR (300 MHz, $CDCl_3$) δ 4.90 (br s, 1H), 3.19 (q, J = 5.8 Hz, 2H), 2.80 (t, J = 6.0 Hz, 2H), 1.43 (s, 11H).

5.3.2. Mono-Boc-1,3-diaminopropane (32)

From **21**, the general procedure afforded the desired product as a clear, pale-yellow viscous oil (0.330 g, 83%): ^{1}H NMR (300 MHz,

$CDCl_3$) δ 4.97 (br s, 1H), 3.21 (q, J = 6.2 Hz, 2H), 2.75 (t, J = 6.6 Hz, 2H), 1.62–1.53 (m, 2H), 1.41 (s, 11H).

5.3.3. Mono-Boc-1,4-diaminobutane (33)

From **22**, the general procedure afforded the desired product as a clear yellow viscous oil (0.443 g, 100% with minor impurities): ^{1}H NMR (300 MHz, $CDCl_3$) δ 4.74 (br s, 1H), 3.10 (q, J = 6.1 Hz, 2H), 2.70 (t, J = 6.7 Hz, 2H), 1.50–1.43 (m, 4H), 1.41 (s, 11H).

5.3.4. Mono-Boc-1,5-diaminopentane (34)

From **23**, the general procedure afforded the desired product as a viscous yellow oil (0.418 g, 90%): ^{1}H NMR (300 MHz, $CDCl_3$) δ 4.56 (br s, 1H), 3.12 (q, J = 6.3 Hz, 2H), 2.71 (t, J = 6.7 Hz, 2H), 1.67–1.28 (m, 17H).

5.3.5. Mono-Boc-1,5-diaminohexane (35)

From **24,** the general procedure afforded the desired product as a yellow semisolid (0.428 g, 86%): ^{1}H NMR (300 MHz, $CDCl_3$) δ 4.54 (br s, 1H), 3.13 (q, J = 6.5 Hz, 2H), 2.70 (t, J = 6.6 Hz, 2H), 1.43 (s, 11H), 1.34–1.30 (m, 8H).

5.3.6. Mono-Boc-1,7-diaminoheptane (36)

From **25**, the general procedure afforded the desired product as a clear, pale-yellow viscous oil (0.387 g, 73%): ^{1}H NMR (500 MHz, $CDCl_3$) δ 4.54 (br s, 1H), 3.20–3.00 (m, 2H), 2.68 (t, J = 7.0 Hz, 2H), 1.62–1.55 (m, 4H), 1.42 (s, 9H), 1.30–1.10 (m, 8H).

5.3.7. Mono-Boc-1,8-diaminooctane (37)

From **26,** the general procedure afforded the product as a colorless semisolid (0.493 g, 91%): ^{1}H NMR (300 MHz, $CDCl_3$) δ 4.50 (br s, 1H), 3.11 (q, J = 6.8 Hz, 2H), 2.70 (t, J = 6.8 Hz, 2H), 1.60–1.50 (m, 4H), 1.44 (s, 11H), 1.40–1.30 (m, 8H).

5.3.8. Mono-Boc-1,9-diaminononane (38)

From **27**, the general procedure afforded the product as a viscous, colorless oil which solidified upon standing (0.437 g, 74%): ^{1}H NMR (300 MHz, $CDCl_3$) δ 4.50 (br s, 1H), 3.13 (q, J = 6.5 Hz, 2H), 2.69 (t, J = 6.8 Hz, 2H), 1.40–1.30 (m, 13H), 1.30–1.20 (m, 12H).

5.3.9. Mono-Boc 1,10-diaminodecane (39)

From **28**, the general procedure afforded the product as a colorless semisolid (0.598 g, 96%): ^{1}H NMR (300 MHz, $CDCl_3$) δ 4.51 (br s, 1H), 3.13 (q, J = 6.5 Hz, 2H), 2.69 (t, J = 6.8 Hz, 2H), 1.50–1.30 (m, 15H), 1.30–1.20 (m, 12H).

5.3.10. Mono-Boc-1,11-diaminoundecane (40)

From **29**, the general procedure afforded the product as a colorless semisolid (0.588 g, 90%): ^{1}H NMR (300 MHz, $CDCl_3$) δ 4.49 (br s, 1H), 3.13 (q, J = 6.7 Hz, 2H), 2.70 (t, J = 6.8 Hz, 2H), 1.60–1.40 (m, 17H), 1.30–1.20 (m, 12H).

5.3.11. Mono-Boc-1,12-diaminododecane (41)

From **30**, the general procedure afforded the product as a colorless semisolid (0.547 g, 79%): ^{1}H NMR (300 MHz, $CDCl_3$) δ 4.50 (br s, 1H), 3.11 (q, J = 5.7 Hz, 2H), 2.70 (t, J = 6.9 Hz, 2H), 1.60–1.20 (m, 31H).

5.4. Preparation of aromathecins

5.4.1. 14-(2′-*tert*-Boc-aminoethyl-1′-aminomethyl)-12*H*-5,11a-diazadibenzo[*b,h*]fluoren-11-one (42)

Compound **19** (0.070 g, 0.210 mmol) was diluted in DMSO (20 mL) and **31** (0.101 g, 0.631 mmol) was dissolved in DMSO (1 mL) and added to the suspension. The mixture was sonicated briefly to break up the starting material and stirred at room temperature for 19 h, poured into H_2O (100 mL), and extracted with $CHCl_3$ (1 × 100 mL, 1 × 60 mL). The organic layers were washed with H_2O (2 × 140 mL, 2 × 280 mL), dried over anhydrous sodium sulfate, and concentrated. The residue was adsorbed onto SiO_2, and purified by flash column chromatography (SiO_2), eluting with 0.4% Et_3N in $CHCl_3$. The obtained solid was further purified by preparative TLC (SiO_2, 1.5% MeOH, and a few drops of Et_3N in $CHCl_3$) to yield a yellow amorphous solid (0.059 g, 62%) after washing with ether: mp 170–173 °C. IR (film) 3436, 2975, 1712, 1655, 1617, 1598, 1502, 1456, 1364, 1171, 753, 687 cm^{-1}; ^{1}H NMR (300 MHz, $CDCl_3$) δ 8.54 (d, J = 8.1 Hz, 1H), 8.25 (dd, J = 12.2 Hz, 8.3 Hz, 2H), 7.79–7.56 (m, 6H), 5.43 (s, 2H), 4.92 (br s, 1H), 4.37 (s, 2H), 3.31 (q, J = 5.6 Hz, 2H), 2.91 (t, J = 5.8 Hz, 2H), 1.68 (s, 1H, under residual solvent peak), 1.42 (s, 9H); ESIMS m/z (rel intensity) 457 (MH^+, 65), 357, (MH^+−Boc, 100). Anal. Calcd for $C_{27}H_{28}N_4O_3{\cdot}0.75H_2O$: C, 68.99; H, 6.33; N, 11.92. Found: C, 68.76; H, 6.51; N, 11.89.

5.4.2. 14-(3′-*tert*-Boc-aminopropyl-1′-aminomethyl)-12*H*-5,11a-diazadibenzo[*b,h*]fluoren-11-one (43)

Compound **19** (0.070 g, 0.210 mmol) was diluted in DMSO (25 mL) and compound **32** (0.110 g, 0.631 mmol) was dissolved in DMSO (1 mL) and added, and the mixture was sonicated briefly to break up the starting material. The mixture was stirred at room temperature for 16 h, poured into H_2O (100 mL), and extracted with $CHCl_3$ (2 × 70 mL, 2 × 40 mL). The organic layers were washed with H_2O (4 × 140 mL), dried over anhydrous sodium sulfate, and concentrated. The residue was adsorbed onto SiO_2, and purified by flash column chromatography (SiO_2), eluting with 0.6% Et_3N in $CHCl_3$. The obtained solid was further purified by preparative TLC (SiO_2, 1.5% MeOH, few drops Et_3N in $CHCl_3$) to yield a yellow amorphous solid (0.061 g, 62%) after washing with ether: mp 145–158 °C. IR (film) 3307, 2975, 1696, 1659, 1622, 1602, 1512, 1365, 1345, 1170, 754, 687 cm^{-1}; ^{1}H NMR (300 MHz, $CDCl_3$) δ 8.56 (d, J = 7.9 Hz, 1H), 8.30 (d, J = 8.5 Hz, 1H), 8.24 (d, J = 8.2 Hz, 1H), 7.79–7.57 (m, 6H), 5.47 (s, 2H), 4.87 (br s, 1H), 4.36 (s, 2H), 3.22 (q, J = 6.4 Hz, 2H), 2.85 (t, J = 6.5 Hz, 2H), 1.75–1.70 (m, 3H), 1.39 (s, 9H); ESIMS m/z (rel intensity) 471 (MH^+, 35), 371, (MH^+−Boc, 100). Anal. Calcd for $C_{28}H_{30}N_4O_3$: C, 71.47; H, 6.43; N, 11.91. Found: C, 71.12; H, 6.64; N, 11.81.

5.4.3. 14-(4′-*tert*-Boc-aminobutyl-1′-aminomethyl)-12*H*-5,11a-diazadibenzo[*b,h*]fluoren-11-one (44)

Compound **19** (0.070 g, 0.210 mmol) was diluted in DMSO (20 mL) and compound **33** (0.119 g, 0.630 mmol) was dissolved in DMSO (2 mL) and added. The mixture was stirred at room temperature for 17 h, poured into H_2O (100 mL), and extracted with $CHCl_3$ (60 mL); additionally, MeOH (70 mL) was added to the organic phase to aid solubility. The organic layer was washed with H_2O (4 × 150 mL), dried over anhydrous sodium sulfate, and concentrated. The obtained residue was adsorbed onto SiO_2 and purified by flash column chromatography (SiO_2), eluting with 0.6% Et_3N in $CHCl_3$, to yield a yellow amorphous solid (0.069 g, 68%) after washing with ether: mp 168–175 °C (dec). IR (film) 3351, 2930, 1693, 1657, 1621, 1601, 1509, 1365, 1250, 1173, 753, 687 cm^{-1}; ^{1}H NMR (300 MHz, $CDCl_3$) δ 8.56 (d, J = 8.0 Hz, 1H), 8.26 (t, J = 8.4 Hz, 1H), 7.79–7.57 (m, 6H), 5.47 (s, 2H), 4.67 (br s, 1H), 4.37 (s, 2H), 3.14 (q, J = 6.0 Hz, 2H), 2.80 (t, J = 6.2 Hz, 2H), 1.59–1.55 (m, 5H), 1.42 (s, 9H); ESIMS m/z (rel intensity) 485 (MH^+, 27), 385, (MH^+−Boc, 100).

5.4.4. 14-(5′-*tert*-Boc-aminopentyl-1′-aminomethyl)-12*H*-5,11a-diazadibenzo[*b,h*]fluoren-11-one (45)

Compound **19** (0.081 g, 0.243 mmol) and compound **34** (0.147 g, 0.729 mmol) were diluted with DMSO (25 mL), and the mixture was stirred at room temperature for 19 h. The reaction mixture was diluted with H_2O (100 mL), and extracted with $CHCl_3$, (2 × 100 mL),

with additional H_2O (100 mL) being added to break up the resultant emulsion. The organic layers were washed with H_2O (3 × 100 mL), dried over anhydrous sodium sulfate, concentrated, adsorbed onto SiO_2, and purified by flash column chromatography (SiO_2), eluting with 0.4% Et_3N in $CHCl_3$ to yield a pale-yellow amorphous solid (0.079 g, 66%) after washing with ether: mp 186–189 °C. IR (film) 3368, 2928, 2856, 1693, 1656, 1619, 1600, 1512, 1453, 1365, 1250, 1172, 835, 752, 686 cm^{-1}; ^1H NMR (300 MHz, $CDCl_3$) δ 8.56 (d, J = 8.0 Hz, 1H), 8.26 (t, J = 8.8 Hz, 2H), 7.78–7.57 (m, 6H), 5.47 (s, 2H), 4.66 (br s, 1H), 4.67 (s, 2H), 3.12 (q, J = 6.2 Hz, 2H), 2.78 (t, J = 7.0 Hz, 2H), 1.60–1.35 (m, 16H); ESIMS m/z (rel intensity) 499 (MH^+, 57), 997, ($2MH^+$ 100).

5.4.5. 14-(6′-*tert*-Boc-aminohexyl-1′-aminomethyl)-12*H*-5,11a-diazadibenzo[*b,h*]fluoren-11-one (46)

Compound **19** (0.070 g, 0.210 mmol) was diluted with DMSO (20 mL) and compound **35** (0.136 g, 0.631 mmol) was dissolved in DMSO (3 mL) and pipetted into the suspension. The mixture was stirred at room temperature for 16 h, poured into H_2O (120 mL) and extracted with $CHCl_3$ (2 × 50 mL, 1 × 30 mL). The organic layers were washed with H_2O (1 × 120 mL, 4 × 100 mL), dried over anhydrous sodium sulfate, concentrated, adsorbed onto SiO_2, and purified by flash column chromatography (SiO_2), eluting with 0.4% Et_3N in $CHCl_3$. The obtained residue was further purified by preparative TLC (SiO_2, 1% MeOH, and a few drops of Et_3N in $CHCl_3$), to yield a pale-yellow amorphous solid (0.055 g, 51%) after washing with ether: mp 99–104 °C. IR (film) 3437, 3360, 3285, 2928, 1705, 1655, 1619, 1601, 1452, 1365, 1172, 835, 752, 685 cm^{-1}; ^1H NMR (300 MHz, $CDCl_3$) δ 8.55 (d, J = 8.1 Hz, 1H), 8.25 (t, J = 8.1 Hz, 2H), 7.80–7.54 (m, 6H), 5.46 (s, 2H), 4.63 (br s, 1H), 4.35 (s, 2H), 3.10 (q, J = 6.3 Hz, 2H), 2.77 (t, J = 7.0 Hz, 2H), 1.60–1.30 (m, 18H); ESIMS m/z (rel intensity), 513, (MH^+, 80), 413 (MH^+−Boc, 100).

5.4.6. 14-(7′-*tert*-Boc-aminoheptyl-1′-aminomethyl)-12*H*-5,11a-diazadibenzo[*b,h*]fluoren-11-one (47)

Compound **19** (0.055 g, 0.165 mmol) was diluted with DMSO (25 mL). Compound **36** (0.114 g, 0.495 mmol) was dissolved in DMSO (2 mL) and added to the suspension. The mixture was stirred at room temperature for 22 h, diluted with $CHCl_3$ (40 mL), and washed with H_2O (4 × 50 mL). The organic phase was dried over anhydrous sodium sulfate, concentrated, and the residue was washed with ether and filtered. The filtrate was diluted with $CHCl_3$ (30 mL) and washed again with H_2O (3 × 20 mL) to remove residual DMSO, before it was dried over anhydrous sodium sulfate, combined with the filtered residue, adsorbed onto SiO_2, and purified by flash column chromatography (SiO_2), eluting with a gradient of $CHCl_3$ to 0.5% MeOH–0.5% Et_3N to yield a yellow amorphous solid that was further purified by preparative TLC (SiO_2, 1.2% MeOH in $CHCl_3$), to yield a pale-yellow amorphous solid (0.039 g, 45%) after washing with ether: mp 97–105 °C. IR (film) 3436, 2926, 2855, 1691, 1655, 1619, 1601, 1512, 1453, 1365, 1252, 1174, 836, 753, 685 cm^{-1}; ^1H NMR (300 MHz, $CDCl_3$) δ 8.58 (d, J = 7.8 Hz, 1H), 8.27 (t, J = 9.4 Hz, 2H), 7.80–7.58 (m, 6H), 5.48 (s, 2H), 4.69 (br s, 1H), 4.37 (s, 2H), 3.10 (q, J = 6.3 Hz, 2H), 2.77 (t, J = 7.0 Hz, 2H), 1.60–1.20 (m, 20H); ESIMS m/z (rel intensity), 527, (MH^+, 78), 427 (MH^+−Boc, 100).

5.4.7. 14-(8′-*tert*-Boc-aminooctyl-1′-aminomethyl)-12*H*-5,11a-diazadibenzo[*b,h*]fluoren-11-one (48)

Compound **19** (0.071 g, 0.213 mmol) was diluted with DMSO (25 mL), and compound **37** was dissolved in DMSO (2 mL) and added to the suspension. The mixture was stirred at room temperature for 16 h, diluted with $CHCl_3$ (40 mL) and washed with H_2O (3 × 50 mL, 1 × 80 mL). The organic phase was dried over anhydrous sodium sulfate, concentrated, adsorbed onto SiO_2, and purified by flash column chromatography (SiO_2), eluting with a gradient of $CHCl_3$–0.5% MeOH in $CHCl_3$. The resultant residue was purified further by preparative TLC (1% MeOH in $CHCl_3$) to yield a yellow amorphous solid (0.048 g, 42%) after washing with ether and hexanes: mp 96–101 °C. IR (film) 3436, 3361, 3287, 2924, 2854, 1684, 1655, 1618, 1600, 1452, 1364, 1250, 1173, 834, 752, 685 cm^{-1}; ^1H NMR (300 MHz, $CDCl_3$) δ 8.56 (d, J = 8.0 Hz, 1H), 8.26 (t, J = 9.1 Hz, 2H), 7.78–7.56 (m, 6H), 5.46 (s, 2H), 4.61 (br s, 1H), 4.36 (s, 2H), 3.12 (q, J = 6.5 Hz, 2H), 2.76 (t, J = 7.1 Hz, 2H), 1.70–1.20 (m, 22H); ESIMS m/z (rel intensity) 541 (MH^+, 32), 441 (MH^+−Boc, 100), 563 (MNa^+, 37).

5.4.8. 14-(9′-*tert*-Boc-aminononyl-1′-aminomethyl)-12*H*-5,11a-diazadibenzo[*b,h*]fluoren-11-one (49)

Compound **19** (0.070 g, 0.210 mmol) was diluted with DMSO (20 mL) and compound **38** (0.163 g, 0.631 mmol) was added as a suspension in DMSO (5 mL). The mixture was stirred at room temperature for 20 h, diluted with H_2O (100 mL) and extracted with $CHCl_3$ (2 × 50 mL, 1 × 30 mL). The organic layers were washed with H_2O (1 × 120 mL, 4 × 100 mL), dried over anhydrous sodium sulfate, concentrated, adsorbed onto SiO_2, and purified by flash column chromatography (SiO_2), eluting with 0.2% Et_3N in $CHCl_3$. The obtained residue was further purified by preparative TLC (SiO_2, 1% MeOH, and few drops of Et_3N in $CHCl_3$), to afford the desired product as a yellow amorphous solid (0.054 g, 47%) after washing with ether: mp 90–98 °C. IR (film) 3438, 3360, 2925, 2854, 1693, 1655, 1618, 1600, 1511, 1452, 1365, 1250, 1173, 836, 752, 685 cm^{-1}; ^1H NMR (300 MHz, $CDCl_3$) δ 8.55 (J = 7.8 Hz, 1H), 8.27 (dd, J = 13.4 Hz, 8.2 Hz), 7.79–7.56 (m, 6H), 5.47 (s, 2H), 4.56 (br s, 1H), 4.38 (s, 2H), 3.10 (q, J = 6.7 Hz, 2H), 2.78 (t, J = 7.1 Hz, 2H), 1.74–1.26 (m, 24H); ESIMS m/z (rel intensity), 555 (MH^+, 100).

5.4.9. 14-(10′-*tert*-Boc-aminodecyl-1′-aminomethyl)-12*H*-5,11a-diazadibenzo[*b,h*]fluoren-11-one (50)

Compound **19** (0.070 g, 0.210 mmol) was diluted with DMSO (20 mL) and compound **39** (0.172 g, 0.630 mmol) was added as a suspension in DMSO (5 mL). The reaction mixture was stirred at room temperature for 17 h, diluted with H_2O (120 mL), and extracted with $CHCl_3$ (2 × 50 mL, 2 × 80 mL, 1 × 30 mL). The organic layers were washed with H_2O (5 × 200 mL), dried over anhydrous sodium sulfate, concentrated, and the resultant residue was adsorbed onto SiO_2 and purified by flash column chromatography (SiO_2) eluting with 0.2% Et_3N in $CHCl_3$. The obtained material was further purified by preparative TLC (0.7% MeOH, and a few drops of Et_3N in $CHCl_3$), to yield a bright pale-yellow amorphous solid (0.062 g, 52%) after washing with ether: mp 88–95 °C. IR (film) 3437, 3285, 2924, 2853, 1703, 1655, 1618, 1600, 1453, 1364, 1172, 834, 752, 685 cm^{-1}; ^1H NMR (300 MHz, $CDCl_3$) δ 8.56 (d, J = 8.0 Hz, 1H), 8.27 (dd, J = 13.6 Hz, 8.4 Hz, 2H), 7.80–7.55 (m, 6H), 5.47 (s, 2H), 4.53 (br s, 1H), 4.37 (s, 2H), 3.10 (q, J = 5.8 Hz, 2H), 2.77 (t, J = 7.0 Hz, 2H), 1.64–1.25 (m, 26H); ESIMS m/z (rel intensity), 569 (MH^+, 46), 1137 ($2MH^+$, 100).

5.4.10. 14-(11′-*tert*-Boc-aminoundecyl-1′-aminomethyl)-12*H*-5,11a diazadibenzo[*b,h*]fluoren-11-one (51)

Compound **19** (0.070 g, 0.210 mmol) and compound **40** (0.180 g, 0.630 mmol) were diluted with DMSO (25 mL) and the mixture was stirred at room temperature for 16 h. The mixture was diluted with H_2O (100 mL), extracted with $CHCl_3$ (2 × 50 mL, 2 × 90 mL, 1 × 50 mL, 1 × 30 mL), and the organic layers were washed with H_2O (5 × 200 mL), before they were dried over anhydrous sodium sulfate, concentrated, adsorbed onto SiO_2, and purified by flash column chromatography (SiO_2), eluting with 0.2% Et_3N in $CHCl_3$, to yield a yellow amorphous solid (0.067 g, 55%) after washing with ether and hexanes: mp 88–100 °C. IR (film) 3436, 3368, 2923, 2853, 1704, 1655, 1618, 1600, 1453, 1365, 1169, 835, 752, 685 cm^{-1}; ^1H NMR (300 MHz, $CDCl_3$) δ 8.58 (d, J = 8.2 Hz, 1H), 8.28 (dd,

J = 13.0 Hz, 8.4 Hz, 2H), 7.82–7.58 (m, 6H), 5.49 (s, 2H), 4.52 (br s, 1H), 4.38 (s, 2H), 3.10 (q, J = 6.6 Hz, 2H), 2.77 (t, J = 7.1 Hz, 2H), 1.59–1.24 (m, 28H); ESIMS *m/z* (rel intensity), 583 (MH^+, 100).

5.4.11. 14-(12′-*tert*-Boc-aminododecyl-1′-aminomethyl)-12*H*-5,11a diazadibenzo[*b,h*]fluoren-11-one (52)

Compound **19** (0.070 g, 0.210 mmol) and compound **41** (0.190 g, 0.631 mmol) were diluted with DMSO (25 mL) and the mixture was stirred at room temperature for 17 h. The mixture was diluted with H_2O (100 mL), extracted with $CHCl_3$ (1 × 50 mL, 3 × 80 mL, 1 × 50 mL) and the organic layers were washed with H_2O (5 × 200 mL), before they were dried over anhydrous sodium sulfate, concentrated, adsorbed onto SiO_2, and purified by flash column chromatography (SiO_2), eluting with 0.2% Et_3N in $CHCl_3$, to yield a pale-yellow amorphous solid (0.088 g, 70%) after partially dissolving in ether and precipitating out with hexanes: mp 81–90 °C. IR (film) 3435, 3369, 2922, 2852, 1689, 1655, 1618, 1600, 1453, 1365, 1168, 634, 752, 685 cm^{-1}; ^1H NMR (300 MHz, $CDCl_3$) δ 8.58 (d, J = 7.7 Hz, 1H), 8.29 (dd, J = 12.6, 7.9 Hz, 2H), 7.81–7.59 (m, 6H), 5.49 (s, 2H), 4.50 (br s, 1H), 4.38 (s, 2H), 3.10 (q, J = 6.7 Hz, 2H), 2.76 (t, J = 7.1 Hz, 2H), 1.57–1.23 (m, 30H); ESIMS *m/z* (rel intensity), 597 (MH^+, 100). Anal. Calcd for $C_{37}H_{48}N_4O_3 \cdot 0.5H_2O$: C, 73.36; H, 8.15; N, 9.25. Found: C, 73.09; H, 8.25; N, 9.23.

5.4.12. 14-(2′-Aminoethyl-1′-aminomethyl)-12*H*-5,11a-diazadibenzo[*b,h*]fluoren-11-one trihydrochloride (53)

Compound **42** (0.050 g, 0.110 mmol) was dissolved in $CHCl_3$ (30 mL). Methanolic HCl (3 M, 10 mL) was added dropwise. The addition was slightly exothermic. The mixture was stirred at room temperature for 2 h and concentrated to yield a red-orange solid after washing with ether and drying in vacuo. The powder was then washed with a solution of $CHCl_3$ (containing several drops of MeOH) to remove residual $Et_3N \cdot HCl$, yielding the desired product as a red powder (0.035 g, 69%) after washing with ether: mp 228–235 °C (dec). IR (KBr) 3400, 2991, 2725, 1651, 1595, 1337, 1156, 770, 684 cm^{-1}; ^1H NMR (300 MHz, D_2O) δ 7.78 (d, J = 8.6 Hz, 1H), 7.65 (s, 2H), 7.52–7.39 (m, 4H), 7.08 (t, J = 6.6 Hz, 1H), 7.00 (s, 1H), 5.12 (s, 2H), 4.64 (s, 2H), 3.65 (t, J = 6.8 Hz, 2H), 3.41 (t, J = 7.0 Hz, 2H); ESIMS *m/z* (rel intensity) 357 (MH^+, 100). Anal. Calcd for $C_{22}H_{23}Cl_3N_4O$: C, 56.73; H, 4.98; N, 12.03. Found: C, 56.90; H, 4.75; N, 11.83.

5.4.13. 14-(3′-Aminopropyl-1′-aminomethyl)-12*H*-5,11a-diazadibenzo[*b,h*]fluoren-11-one trihydrochloride (54)

Compound **43** (0.052 g, 0.111 mmol) was dissolved in $CHCl_3$ (30 mL). Methanolic HCl (3 M, 10 mL) was added dropwise. The mixture was stirred at room temperature for 2 h and concentrated to yield a red-orange solid (0.043 g, 82%) after washing with ether and drying in vacuo: mp 232–240 °C (dec). IR (KBr) 3435, 2922, 1659, 1623, 1601, 1479, 1334, 762, 686 cm^{-1}; ^1H NMR (300 MHz, D_2O) δ 7.75 (d, J = 8.3 Hz, 1H), 7.61 (s, 2H), 7.52–7.41 (m, 4H), 7.04–6.96 (m, 2H), 5.10 (s, 2H), 4.60 (s, 2H), 3.38 (t, J = 7.9 Hz, 2H), 3.10 (t, J = 7.4 Hz, 2H), 2.20–2.00 (m, 2H); ESIMS *m/z* (rel intensity) 371(MH^+, 100). Anal. Calcd for $C_{23}H_{25}Cl_3N_4O$: C, 57.57; H, 5.25; N, 11.68. Found: C, 57.91; H, 5.24; N, 11.72.

5.4.14. 14-(4′-Aminobutyl-1′-aminomethyl)-12*H*-5,11a-diazadibenzo[*b,h*]fluoren-11-one trihydrochloride (55)

Compound **44** (0.055 g, 0.113 mmol) was dissolved in $CHCl_3$ (30 mL). Methanolic HCl (3 M, 10 mL) was added dropwise. The mixture was stirred at room temperature for 2 h and concentrated to yield a red-orange solid (0.050 g, 90%) after washing with ether and drying in vacuo: mp 222–228 °C (dec). IR (KBr) 3401, 2928, 1657, 1596, 1476, 1334, 762, 681 cm^{-1}; ^1H NMR (300 MHz, D_2O) δ 7.72 (d, J = 8.2 Hz, 1H), 7.60–7.45 (m, 3H), 7.36–7.32 (m, 3H), 7.10–7.00 (m, 1H), 6.86 (s, 1H). 5.05 (s, 2H), 4.55 (s, 2H), 3.33 (t, J = 6.8 Hz, 2H), 3.05 (t, J = 7.6 Hz, 2H), 1.90–1.70 (m, 4H); ESIMS *m/z* (rel intensity) 385 (MH^+, 100). Anal. Calcd for $C_{24}H_{27}Cl_3N_4O \cdot H_2O$: C, 56.31; H, 5.71; N, 10.95. Found: C, 56.07; H, 5.44; N, 10.58.

5.4.15. 14-(5′-Aminopentyl-1′-aminomethyl)-12*H*-5,11a-diazadibenzo[*b,h*]fluoren-11-one trihydrochloride (56)

Compound **45** (0.065 g, 0.130 mmol) was diluted in $CHCl_3$ (40 mL) and filtered to remove particulate matter. Methanolic HCl (3 M, 10 mL) was added dropwise, and the dark red mixture was stirred for 2 h at room temperature and concentrated to provide a bright red amorphous solid (0.056 g, 86%) after washing with ether and drying in vacuo: mp 245–251 °C (dec). IR (KBr) 3399, 2929, 1654, 1474, 1336, 1217, 766, 683 cm^{-1}; ^1H NMR (300 MHz, D_2O) δ 7.75–7.45 (m, 7H), 7.20–7.02 (m, 2H), 5.12 (s, 2H), 4.57 (s, 2H), 3.27 (t, J = 6.9 Hz, 2H), 2.98 (t, J = 6.4 Hz, 2H), 1.80–1.60 (m, 4H), 1.50–1.40 (m, 2H); ESIMS *m/z* (rel intensity). 399 (MH^+, 100). Anal. Calcd for $C_{25}H_{29}Cl_3N_4O \cdot 2H_2O$: C, 55.21; H, 6.12; N, 10.30. Found: C, 55.29; H, 5.97; N, 10.20.

5.4.16. 14-(6′-Aminohexyl-1′-aminomethyl)-12*H*-5,11a-diazadibenzo[*b,h*]fluoren-11-one trihydrochloride (57)

Compound **46** (0.050 g, 0.097 mmol) was dissolved in $CHCl_3$ (30 mL) and methanolic HCl (3 M, 10 mL) was added dropwise. The orange cloudy mixture was stirred at room temperature for 2 h and concentrated to afford a dark red amorphous solid (0.043 g, 85%) after washing with ether and drying in vacuo: mp 230–235 °C. IR (KBr) 3412, 2928, 1657, 1622, 1596, 1478, 1337, 765, 682 cm^{-1}; ^1H NMR (300 MHz, D_2O) δ 7.72 (d, J = 8.4 Hz, 1H), 7.60 (s, 2H), 7.51–7.42 (m, 4H), 7.06 (t, J = 5.4 Hz, 1H), 6.95 (s, 1H), 5.08 (s, 2H), 4.54 (s, 2H), 3.25 (t, J = 7.7 Hz, 2H), 2.97 (t, J = 7.4 Hz, 2H), 1.80–1.60 (m, 4H), 1.30–1.40 (m, 4H); ESIMS *m/z* (rel intensity) 413 (MH^+, 100). Anal. Calcd for $C_{26}H_{31}Cl_3N_4O \cdot H_2O$: C, 57.84; H, 6.16; N, 10.38. Found: C, 57.53; H, 6.48; N, 10.03.

5.4.17. 14-(7′-Aminoheptyl-1′-aminomethyl)-12*H*-5,11a-diazadibenzo[*b,h*]fluoren-11-one trihydrochloride (58)

Compound **47** (0.035 g, 0.066 mmol) was diluted with benzene (25 mL) and methanolic HCl (3 M, 10 mL) was added dropwise, upon which the solution became dark red. The mixture was heated at reflux for 3 h, cooled, and concentrated to yield a bright orange solid (0.030 g, 85%) after washing with ether: mp 208–215 °C (dec). IR (KBr) 3400, 2929, 1657, 1620, 1600, 1457, 1340, 1132, 764, 687 cm^{-1}; ^1H NMR (300 MHz, D_2O) δ 7.75–7.69 (m, 3H), 7.58–7.48 (m, 4H), 7.20–7.08 (m, 2H), 5.13 (s, 2H), 4.56 (s, 2H), 3.23 (t, J = 8.1 Hz, 2H), 2.95 (t, J = 7.7 Hz, 2H), 1.80–1.50 (m, 4H), 1.30–1.20 (m, 6H); ESIMS *m/z* (rel intensity) 427 (MH^+, 100). Anal. Calcd for $C_{27}H_{33}Cl_3N_4O \cdot 1.5H_2O$: C, 57.60; H, 6.45; N, 9.95. Found: C, 57.47; H, 6.49; N, 9.64.

5.4.18. 14-(8′-Aminooctyl-1′-aminomethyl)-12*H*-5,11a-diazadibenzo[*b,h*]fluoren-11-one trihydrochloride (59)

Compound **48** (0.042 g, 0.078 mmol) was dissolved in $CHCl_3$ (30 mL) and methanolic HCl (3 M, 10 mL) was added dropwise, upon which the solution became dark orange-red. The mixture was stirred at room temperature for 2 h and concentrated to yield a dark red flaky solid (0.036, 85%) after washing with ether and drying in vacuo: mp 200–203 °C (dec). IR (KBr) 3401, 2929, 2856, 1758, 1656, 1597, 1619, 1479, 1338, 1135, 764, 688 cm^{-1}; ^1H NMR (300 MHz, D_2O) 7.70 δ (d, J = 8.1 Hz, 1H), 7.60–7.38 (m, 6H), 7.04–7.02 (m, 1H), 6.89 (s, 1H), 5.04 (s, 2H), 4.50 (s, 2H), 3.22 (t, J = 7.6 Hz, 2H), 2.94 (t, J = 7.3 Hz, 2H), 1.80–1.50 (m, 4H), 1.30–1.20 (m, 8H); ESIMS *m/z* (rel intensity) 441 (MH^+, 100). Anal. Calcd for $C_{28}H_{35}Cl_3N_4O \cdot H_2O$: C, 59.21; H, 6.57; N, 9.86. Found: C, 59.03; H, 6.81; N, 9.78.

5.4.19. 14-(9′-Aminononyl-1′-aminomethyl)-12*H*-5,11a-diazadibenzo[*b*,*h*]fluoren-11-one trihydrochloride (60)

Compound **49** (0.046 g, 0.083 mmol) was dissolved in $CHCl_3$ (20 mL) and methanolic HCl (3 M, 10 mL) was added dropwise. The mixture was stirred for 2 h 20 min at room temperature, concentrated, and azeotroped with benzene, to afford a bright red amorphous solid (0.038 g, 82%) after washing with ether and drying in vacuo: mp 192–196 °C (dec). IR (KBr) 3414, 2928, 2854, 1657, 1622, 1599, 1478, 1336, 761, 688 cm^{-1}; ^1H NMR (300 MHz, D_2O) δ 7.73–7.65 (m, 3H), 7.52–7.45 (m, 4H), 7.20–7.00 (m, 2H), 5.10 (s, 2H), 4.53 (s, 2H), 3.21 (t, J = 6.9 Hz, 2H), 2.92 (J = 7.2 Hz, 2H), 1.70–1.50 (m, 4H), 1.40–1.20 (m, 10H); ESIMS *m/z* (rel intensity) 455 (MH^+, 100). Anal. Calcd for $C_{29}H_{37}Cl_3N_4O$: C, 61.76; H, 6.61; N, 9.93. Found: C, 61.50; H, 7.00; N, 9.71.

5.4.20. 14-(10′-Aminodecyl-1′-aminomethyl)-12*H*-5,11a-diazadibenzo[*b*,*h*]fluoren-11-one trihydrochloride (61)

Compound **50** (0.056 g, 0.096 mmol) was dissolved in $CHCl_3$ (30 mL) and methanolic HCl (3 M, 10 mL) was added dropwise. The addition was slightly exothermic. The mixture was stirred for 2 h at room temperature and concentrated to yield a red amorphous solid (0.049 g, 87%) after washing with ether and drying in vacuo: mp 185–190 °C (dec). IR (KBr) 3433, 2925, 2854, 1657, 1622, 1599, 1469, 1335, 764, 688 cm^{-1}; ^1H NMR (300 MHz, D_2O) δ 7.75–7.69 (m, 3H), 7.56–7.49 (m, 4H), 7.15–7.08 (m, 2H), 5.13 (s, 2H), 4.56 (s, 2H), 3.21 (t, J = 7.4 Hz, 2H), 2.91 (t, J = 7.5 Hz, 2H), 1.70–1.50 (m, 4H), 1.40–1.20 (bm, 12H); ESIMS *m/z* (rel intensity) 469 (MH^+, 100). Anal. Calcd for $C_{30}H_{39}Cl_3N_4O{\cdot}0.6H_2O$: C, 61.19; H, 6.88; N, 9.51. Found: C, 60.97; H, 7.16; N, 9.30.

5.4.21. 14-(11′-Aminoundecyl-1′-aminomethyl)-12*H*-5,11a-diazadibenzo[*b*,*h*]fluoren-11-one trihydrochloride (62)

Compound **51** (0.056 g, 0.097 mmol) was dissolved in $CHCl_3$ (30 mL) and methanolic HCl (3 M, 10 mL) was added dropwise. The reaction was slightly exothermic. The mixture was stirred for 2 h at room temperature and concentrated to yield a red-orange amorphous solid (0.052 g, 91%) after washing with ether and drying in vacuo: mp 183–188 °C (dec). IR (KBr) 3431, 2925, 2853, 1657, 1622, 1601, 1469, 1336, 762, 688 cm^{-1}; ^1H NMR (300 MHz, D_2O) δ 7.75–7.52 (m, 7H), 7.19–7.13 (m, 2H), 5.16 (s, 2H), 4.58 (s, 2H), 3.19 (t, J = 6.2 Hz, 2H), 2.91–2.85 (m, 2H), 1.70–1.50 (m, 4H), 1.40–1.10 (m, 14H); ESIMS *m/z* (rel intensity) 483 (MH^+, 100). Anal. Calcd for $C_{31}H_{41}Cl_3N_4O{\cdot}0.5H_2O$: C, 61.95; H, 7.04; N, 9.32. Found: C, 61.88; H, 7.31; N, 9.10.

5.4.22. 14-(12′-Aminododecyl-1′-aminomethyl)-12*H*-5,11a-diazadibenzo[*b*,*h*]fluoren-11-one trihydrochloride (63)

Compound **52** (0.069 g, 0.115 mmol) was dissolved in $CHCl_3$ (30 mL) and methanolic HCl (3 M, 10 mL) was added dropwise. The reaction mixture was stirred at room temperature for 2 h and concentrated to yield a bright red amorphous solid (0.064 g, 92%) after washing with ether and drying in vacuo: mp 200–204 °C (dec). IR (KBr) 3409, 2924, 2851, 1657, 1619, 1598, 1467, 1337, 764, 688 cm^{-1}; ^1H NMR (300 MHz, D_2O, 60 °C) δ 7.98–7.81 (m, 4H), 7.72 (t, J = 7.8 Hz, 3H), 7.43–7.37 (m, 2H), 5.29 (s, 2H), 4.71 (s, 2H), 3.23 (t, J = 7.6 Hz, 2H), 3.02–2.92 (m, 2H), 1.71–1.56 (m, 4H), 1.30–1.15 (m, 16H); ESIMS *m/z* (rel intensity), 497, (MH^+, 100). Anal. Calcd for $C_{32}H_{43}Cl_3N_4O{\cdot}H_2O$: C, 63.42; H, 7.15; N, 9.24; Cl, 17.55. Found: C, 63.06; H, 7.48; N, 9.12; Cl, 17.17.

5.5. Topoisomerase I-mediated DNA cleavage reactions

Human recombinant top1 was purified from Baculovirus as previously described.[56] DNA cleavage reactions were prepared as previously reported[30] (for review see[57]) with the exception of the DNA substrate. Briefly, a 117-bp DNA oligonucleotide (Integrated DNA Technologies) encompassing the previous identified top1 cleavage sites identified in the 161-bp fragment from pBluescript SK(−) phagemid DNA was employed. This 117-bp oligonucleotide contains a single 5′-cytosine overhang, which was 3′-end labeled by fill-in reaction with [α-^{32}P]-dGTP in React 2 buffer (50 mM Tris–HCl, pH 8.0, 100 mM $MgCl_2$, 50 mM NaCl) with 0.5 units of DNA polymerase I (Klenow fragment, New England BioLabs). Unincorporated ^{32}P-dGTP was removed using mini Quick Spin DNA columns (Roche, Indianapolis, IN), and the eluate containing the 3′-end-labeled DNA substrate was collected. Approximately 2 nM of radiolabeled DNA substrate was incubated with recombinant top1 in 20 μL of reaction buffer [10 mM Tris–HCl (pH 7.5), 50 mM KCl, 5 mM $MgCl_2$, 0.1 mM EDTA, and 15 μg/ml BSA] at 25 °C for 20 min in the presence of various concentrations of compounds. The reactions were terminated by adding SDS (0.5% final concentration) followed by the addition of two volumes of loading dye (80% formamide, 10 mM sodium hydroxide, 1 mM sodium EDTA, 0.1% xylene cyanol, and 0.1% bromphenol blue). Aliquots of each reaction were subjected to 20% denaturing PAGE. Gels were dried and visualized by using a Phosphoimager and ImageQuant software (Molecular Dynamics). For simplicity, cleavage sites were numbered as previously described in the 161-bp fragment.[56]

5.6. Modeling studies

The crystal structure of topotecan in complex with top1 and a short DNA fragment were downloaded from the Protein Data Bank (PDB code 1K4T).[8] An atom of Hg and one molecule of PEG were deleted. Hydrogens were added and minimized by the Powell method, using the MMFF94s force field and MMFF94 charges. Analogues of aromathecins and indenoisoquinolines were constructed in Sybyl 8.1 (Tripos, Inc.). Fixed positive charges were assigned to amines using Sybyl atom types, and the structures were energy minimized using a conjugate gradient method, MMFF94s force field, and MMFF94 charges. The structure of the ligand was aligned onto topotecan using the 'fit atoms' function. In the case of **64**, the alignment was based on both the overlay of the crystal structures 1K4T and 1SC7, and on earlier overlays of indenoisoquinolines and aromathecins.[8,30] The aligned ligand was merged into the crystal structure, and the structure of topotecan was deleted. This new ternary complex was re-subjected to energy minimization using a standard Powell method, the MMFF94s force field, and MMFF94 charges, converging to termination at 0.05 kcal/mol Å, with a distance-dependent dielectric function. The structure of the ligand and a sphere with a radius of 5 Å were allowed to move during the minimization, and the surrounding structures were frozen in an aggregate.

Acknowledgments

This work was made possible by the National Institutes of Health (NIH) through support with Research Grant UO1 CA89566. This work was also made possible by the Lynn and McKeehan Fellowships (Purdue University, M.A.C.), and by the CIC/SROP program (Purdue University, B.C.). This research was supported in part by the Intramural Research Program of the NIH, National Cancer Institute, Center for Cancer Research. M.A.C. wishes to thank Drs. Andrew Morrell, Karl Wood, and Huaping Mo for their assistance and insight.

References and notes

1. Pommier, Y. *Nat. Rev. Cancer* **2006**, *6*, 789.
2. Wang, J. C. *Nat. Rev. Mol. Cell Biol.* **2002**, *3*, 430.
3. Husain, I.; Mohler, J. L.; Seigler, H. F.; Besterman, J. M. *Cancer Res.* **1994**, *54*, 539.
4. Giovanella, B. C.; Stehlin, J. S.; Wall, M. E.; Wani, M. C.; Nicholas, A. W.; Liu, L. F.; Silber, R.; Potmesil, M. *Science* **1989**, *246*, 1046.

5. Wall, M. E.; Wani, M. C.; Cook, C. E.; Palmer, K. H.; McPhail, A. T.; Sim, G. A. *J. Am. Chem. Soc.* **1966**, *88*, 3888.
6. Hsiang, Y. H.; Hertzberg, R.; Hecht, S.; Liu, L. F. *J. Biol. Chem.* **1985**, *260*, 14873.
7. Staker, B. L.; Hjerrild, K.; Feese, M. D.; Behnke, C. A.; Burgin, A. B., Jr.; Stewart, L. *Proc. Natl. Acad. Sci. U.S.A.* **2002**, *99*, 15387.
8. Staker, B. L.; Feese, M. D.; Cushman, M.; Pommier, Y.; Zembower, D.; Stewart, L.; Burgin, A. *J. Med. Chem.* **2005**, *48*, 2336.
9. Li, T. K.; Liu, L. F. *Annu. Rev. Pharmacol. Toxicol.* **2001**, *41*, 53.
10. Nakagawa, H.; Saito, H.; Ikegami, Y.; Aida-Hyugaji, S.; Sawada, S.; Ishikawa, T. *Cancer Lett.* **2006**, *234*, 81.
11. Pommier, Y.; Pourquier, P.; Urasaki, Y.; Wu, J.; Laco, G. *Drug Resist. Updat.* **1999**, *2*, 307.
12. Chrencik, J. E.; Staker, B. L.; Burgin, A. B., Jr.; Pourquier, P.; Pommier, Y.; Stewart, L.; Redinbo, M. R. *J. Mol. Biol.* **2004**, *339*, 773.
13. Teicher, B. A. *Biochem. Pharmacol.* **2008**, *75*, 1262.
14. Schaeppi, U.; Fleischman, R.; Cooney, D. W. (NSC-100880), *Cancer Chemother. Rep.* **1974**, *58*, 25.
15. Jaxel, C.; Kohn, K. W.; Wani, M. C.; Wall, M. E.; Pommier, Y. *Cancer Res.* **1989**, *49*, 1465.
16. Hsiang, Y.-H.; Liu, L. F.; Wall, M. E.; Wani, M. C.; Nicholas, A. W.; Manikumar, G.; Kirschenbaum, S.; Silber, R.; Potmesil, M. *Cancer Res.* **1989**, *49*, 4385.
17. Luzzio, M. J.; Besterman, J. M.; Emerson, D. L.; Evans, M. G.; Lackey, K.; Leitner, P. L.; McIntyre, G.; Morton, B.; Myers, P. L.; Peel, M.; Sisco, J. M.; Sternbach, D. D.; Tong, W.; Truesdale, A.; Uehling, D. E.; Vuong, A.; Yates, I. *J. Med. Chem.* **1995**, *38*, 395.
18. Haas, N. B.; LaCreta, F. P.; Walczak, J.; Hudes, G. R.; Brennan, J. M.; Ozols, R. F.; O'Dwyer, P. J. *Cancer Res.* **1994**, *54*, 1220.
19. Cagir, A.; Jones, S. H.; Gao, R.; Eisenhauer, B. M.; Hecht, S. M. *J. Am. Chem. Soc.* **2003**, *125*, 13628.
20. Bailly, C.; Riou, J. F.; Colson, P.; Houssier, C.; Rodrigues-Pereira, E.; Prudhomme, M. *Biochemistry* **1997**, *36*, 3917.
21. Saif, M. W.; Diasio, R. B. *Clin. Colorectal Cancer* **2005**, *5*, 27.
22. Kohlhagen, G.; Paull, K. D.; Cushman, M.; Nagafuji, P.; Pommier, Y. *Mol. Pharm.* **1998**, *54*, 50.
23. Nagarajan, M.; Morrell, A.; Fort, B. C.; Meckley, M. R.; Antony, S.; Kohlhagen, G.; Pommier, Y.; Cushman, M. *J. Med. Chem.* **2004**, *47*, 5651.
24. Nagarajan, M.; Morrell, A.; Ioanoviciu, A.; Antony, S.; Kohlhagen, G.; Hollingshead, M.; Pommier, Y.; Cushman, M. *J. Med. Chem.* **2006**, *49*, 6283.
25. Antony, S.; Jayaraman, M.; Laco, G.; Kohlhagen, G.; Kohn, K. W.; Cushman, M.; Pommier, Y. *Cancer Res.* **2003**, *63*, 7428.
26. Antony, S.; Agama, K. K.; Miao, Z.-H.; Takagi, K.; Wright, M. H.; Robles, A. I.; Varticovski, L.; Nagarajan, M.; Morrell, A.; Cushman, M.; Pommier, Y. *Cancer Res.* **2007**, *67*, 10397.
27. Cheng, K.; Rahier, N. J.; Eisenhauer, B. M.; Gao, R.; Thomas, S. J.; Hecht, S. M. *J. Am. Chem. Soc.* **2005**, *127*, 838.
28. Xiao, X.; Antony, S.; Pommier, Y.; Cushman, M. *J. Med. Chem.* **2006**, *49*, 1408.
29. Fox, B. M.; Xiao, X.; Antony, S.; Kohlhagen, G.; Pommier, Y.; Staker, B. L.; Stewart, L.; Cushman, M. *J. Med. Chem.* **2003**, *46*, 3275.
30. Cinelli, M. A.; Morrell, A.; Dexheimer, T.; Scher, E.; Pommier, Y.; Cushman, M. *J. Med. Chem.* **2008**, *51*, 4609.
31. Morrell, A.; Placzek, M. S.; Steffen, J. D.; Antony, S.; Agama, K.; Pommier, Y.; Cushman, M. *J. Med Chem.* **2007**, *50*, 2040.
32. Nagarajan, M.; Xiao, X.; Antony, S.; Kohlhagen, G.; Pommier, Y.; Cushman, M. *J. Med. Chem.* **2003**, *46*, 5712.
33. Dallavalle, S.; Giannini, G.; Alloatti, D.; Casati, A.; Marastoni, A.; Musso, L.; Merlini, L.; Morini, G.; Penco, C.; Pisano, C.; Tinelli, S.; De Cesare, M.; Beretta, G. L.; Zunino, F. *J. Med. Chem.* **2006**, *49*, 5177.
34. Ohara, K.; Smietana, M.; Restouin, A.; Mollard, S.; Borg, J.-P.; Collette, Y.; Vasseur, J.-J. *J. Med. Chem.* **2007**, *50*, 6465.
35. Delcros, J.-G.; Tomasi, S.; Carrington, S.; Martin, B.; Renault, J.; Blagbrough, I. S.; Uriac, P. *J. Med. Chem.* **2002**, *45*, 5098.
36. Babjak, M.; Kanazawa, A.; Anderson, R. J.; Greene, A. E. *Org. Biomol. Chem.* **2006**, *4*, 407.
37. Grillet, F.; Baumlová, B.; Prévost, G.; Constant, J.-F.; Chaumeron, S.; Bigg, C. H.; Greene, A. E.; Kanazawa, A. *Bioorg. Med. Chem. Lett.* **2008**, *18*, 2143.
38. Shamma, M.; Novak, L. *Tetrahedron* **1969**, *25*, 2275.
39. Houghton, P. G.; Humphrey, G. R.; Kennedy, D. J.; Roberts, D. C.; Wright, S. H. B. *J. Chem. Soc., Perkin Trans. 1* **1993**, 1421.
40. Sloan, K. B.; Koch, S. A. M. *J. Org. Chem.* **1983**, *48*, 635.
41. Sugasawa, T.; Toyoda, T.; Adachi, M.; Sasakura, K. *J. Am. Chem. Soc.* **1978**, *100*, 4842.
42. Sugasawa, T.; Adachi, M.; Sakasura, K.; Kitagawa, A. *J. Org. Chem.* **1979**, *44*, 578.
43. Skehan, P.; Storeng, R.; Scudiero, D.; Monks, A.; McMahon, J. *J. Natl. Cancer Inst.* **1990**, *82*, 1107.
44. Boyd, M. R.; Paull, K. D. *Drug Dev. Res.* **1995**, *34*, 91.
45. Nagarajan, M.; Morrell, A.; Antony, S.; Kohlhagen, G.; Agama, K.; Pommier, Y.; Ragazzon, P.; Garbett, N. C.; Chaires, J. B.; Hollingshead, M.; Cushman, M. *J. Med. Chem.* **2006**, *49*, 5129.
46. Wunz, T. P.; Craven, M. T.; Karol, M. D.; Hill, C.; Remers, W. A. *J. Med. Chem.* **1990**, *33*, 1459.
47. Denny, W. A. *Curr. Med. Chem.* **2002**, *9*, 1655.
48. Ioanoviciu, A.; Antony, A.; Pommier, Y.; Staker, B. L.; Stewart, L.; Cushman, M. *J. Med. Chem.* **2005**, *48*, 4803.
49. Marchand, C.; Antony, S.; Kohn, K. W.; Cushman, M.; Ioanoviciu, A.; Staker, B. L.; Burgin, A. B.; Stewart, L.; Pommier, Y. *Mol. Cancer. Ther.* **2006**, *5*, 287.
50. Paull, K. D.; Shoemaker, R. H.; Hodes, L.; Monks, A.; Scudiero, D. A.; Rubinstein, L.; Plowman, J.; Boyd, M. R. *J. Natl. Cancer. Inst.* **1989**, *81*, 1088.
51. Paull, K. D.; Hamel, E.; Malspeis, L. In *Cancer Chemotherapeutic Agents*; Foye, W. O., Ed.; American Chemical Society: Washington, DC, 1995; p 9.
52. Porter, C. W.; Miller, J.; Bergeron, R. J. *Cancer Res.* **1984**, *44*, 126.
53. Morrell, A.; Placzek, M.; Parmley, S.; Grella, B.; Antony, S.; Pommier, Y.; Cushman, M. *J. Med. Chem.* **2007**, *50*, 4388.
54. Sharma, L.; Tsai, Y.-C.; Liu, A. A.; Liu, L. F.; LaVoie, E. J. *Eur. J. Med. Chem.* **2009**, *44*, 1471.
55. Satyanarayana, M.; Feng, W.; Cheng, L.; Liu, A. A.; Tsai, Y.-C.; Liu, L. F.; LaVoie, E. J. *Bioorg. Med. Chem.* **2008**, *16*, 7824.
56. Pourquier, P.; Ueng, L.-M.; Fertala, J.; Wang, D.; Park, H.-K.; Essigmann, J. M.; Bjornsti, M.-A.; Pommier, Y. *J. Biol. Chem.* **1999**, *274*, 8516.
57. Dexheimer, T. S.; Pommier, Y. *Nat. Protocols* **2008**, *3*, 1736.